Quantitative measurements of the generation of hydroxyl radicals by soot particles in a surrogate lung fluid

Heejung Jung[a,b], Bing Guo[a], Cort Anastasio[b,*], Ian M. Kennedy[a]

[a]*Department of Mechanical & Aeronautical Engineering, University of California, Davis, One Shields Avenue, Davis, CA 95616, USA*
[b]*Department of Land, Air & Water Resources, University of California, Davis, One Shields Avenue, Davis, CA 95616, USA*

Abstract

Epidemiological and toxicological studies have shown a relation between the inhalation of atmospheric particles and adverse cardiopulmonary health effects. The generation of reactive oxygen species (ROS) by particles is one current hypothesis for their toxic effects. Thus a quantitative measurement of ROS is important since that will be an index to assess the oxidative stress that particles may cause in the lung. We have developed a technique to quantitatively and specifically measure $^\bullet$OH (the strongest biological ROS) in an aqueous, buffered extract solution as a surrogate lung fluid (SLF). Using this technique we quantitatively measured $^\bullet$OH formation in SLF containing hydrogen peroxide (HOOH) for samples of flame soot particles, carbon black, and ambient fine particles (PM2.5). We have found that $^\bullet$OH is formed by flame soot, independent of transition metals, with a dose-dependent linear response that depends upon HOOH concentration. Experiments with carbon black revealed that its mass-normalized $^\bullet$OH generation was ~10 times lower than that of flame soot, suggesting that carbon black is not a good surrogate for soot particles in health effect studies, at least in terms of oxidative stress. Mass-normalized $^\bullet$OH generation by ambient PM2.5 was 6–30 times larger than that of flame soot. While much of the PM2.5 reactivity was suppressed by pretreating samples with a transition metal chelator, there was a significant fraction of reactivity which was not affected. Our results suggest that the in vivo generation of free radicals, specifically $^\bullet$OH, by inhalation of PM2.5 is partially due to carbonaceous soot as well as transition metals.
© 2005 Elsevier Ltd. All rights reserved.

Keywords: Reactive oxygen species (ROS); Transition metal; Health effect; Oxidative stress; Soot; PM2.5; Combustion

1. Introduction

Epidemiological studies have shown that inhalation of atmospheric particles can cause pulmonary disease, cardiovascular damage, and mortality, although the particles responsible for this toxicity, and the mechanisms of toxicity, are largely unknown (Dockery et al., 1993; Samet et al., 2000). In large urban areas fine carbon particles account for 30–50% of the fine particle mass (Gray et al., 1986; Puxbaum and Wopenka, 1984). These carbonaceous particles mostly originate from combustion sources such as diesel engines, which account for 40–50% of total fine carbon aerosol in Los Angeles (Gray and Cass, 1998), and from coal combustion. While these combustion-generated carbonaceous aerosols are associated with adverse health effects through epidemiological studies (Cohen and

*Corresponding author. Tel.: +1 530 754 6095; fax: +1 530 752 1552.

E-mail address: canastasio@ucdavis.edu (C. Anastasio).

Higgins, 1995; McClellan, 1987), the biological mechanisms for toxicity are not well known (Dellinger et al., 2000). One of the reasons it is difficult to understand the mechanism of toxicity for combustion-generated particles is that these aerosols have a wide variety of physical and chemical properties, including particle number, size, surface area, and chemical composition.

One current hypothesis is that particles exert their toxic effects through the formation of reactive oxygen species (ROS) that can cause oxidative stress (Dellinger et al., 2001; Shi et al., 2003). Indeed, prior in vivo and in vitro studies have shown that combustion-generated particles can lead to the generation of oxidants within lung fluid and cells, which can damage the cell and eventually cause adverse health effects (Li et al., 2003; Sagai et al., 2000). These ROS include superoxide ($^{\bullet}O_2^-$), hydrogen peroxide (HOOH), and hydroxyl radical ($^{\bullet}OH$). The $^{\bullet}OH$ is one of the most strongly oxidizing biological radicals, as it reacts rapidly with most biological molecules and can damage cells and DNA (Imlay et al., 1988; Imlay and Linn, 1988).

The formation of $^{\bullet}OH$ by ambient particles such as PM2.5 has been measured in prior studies, but not in a quantitative manner. For example, Valavanidis et al. (2000) examined ambient particulate matter (PM), diesel and gasoline exhaust particles by electron paramagnetic resonance (EPR) and found that all three types of particles could generate $^{\bullet}OH$ in the presence of HOOH. Shi et al. (2003) examined ambient PM using EPR and found that the particle-mediated generation of $^{\bullet}OH$ in the presence of HOOH was correlated with the Cu content of the PM. Han et al. (2001) indirectly measured $^{\bullet}OH$ generation in mice lungs after intratracheal instillation of diesel exhaust particles using EPR, providing the first evidence of particle-mediated $^{\bullet}OH$ generation in the lungs of living mice. While these studies are important, they are somewhat limited by the fact that EPR gives $^{\bullet}OH$ amounts only in "arbitrary units", which can be compared within a given study but are not quantitative or transferable to other studies.

Donaldson et al. (1997) have semi-quantitatively measured $^{\bullet}OH$ formation from one sample of atmospheric particles using salicylic acid as a radical trap and measuring the resulting stable dihydroxybenzoic acid (DHBA) product. However, because they assumed that the yield of DHBA from the reaction of $^{\bullet}OH$ with salicylic acid was unity, they

might have underestimated the amount of $^{\bullet}OH$ formed. On the other hand, their result might be biased high since they extracted particles by sonication, a process which can generate $^{\bullet}OH$ artificially based on results we describe in this paper.

Many of the past studies of $^{\bullet}OH$ generation by atmospheric particles have focused on transition metal-mediated pathways. In particular, iron has been studied because of its great abundance in ambient particles and its ability to form $^{\bullet}OH$ via the Fenton reaction (Winterbourn, 1995):

$$Fe(II) + HOOH \rightarrow Fe(III) + {}^{\bullet}OH + OH^-. \qquad (1)$$
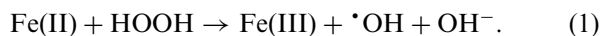
Using synthesized metal-coated carbon black particles, Shi et al. (2003) have shown with EPR that, on a mass-normalized basis, particles coated with Cu and V generate more $^{\bullet}OH$ than Fe, Ni or Zn. van Maanen et al. (1999) and Shi et al. (2003) have also found that there is a correlation between the ability of ambient PM or coal fly ash to generate $^{\bullet}OH$ and the Fe or Cu content, respectively.

On the other hand, a number of studies have found that inhaled carbonaceous soot can also increase oxidative stress. Stone et al. (1998) found ultrafine carbon black exhibits greater free radical activity than fine carbon black on A549 human type-II alveolar epithelial cells, apparently because of the greater particle surface area for a given mass. Brown et al. (2000) reported increased inflammation in the lung of rats after instillation of ultrafine carbon black, compared to that from fine carbon black, and this difference could not be explained by soluble transition metals released from the particle surfaces.

While past studies have shown that $^{\bullet}OH$ is generated by a wide range of ambient and combustion particles, there have been no fully quantitative measures of $^{\bullet}OH$ generation by PM. However, it is important to quantify the formation of ROS such as $^{\bullet}OH$ by particles in order to assess and compare the oxidative stress that a variety of particles pose to the lung. To address this issue we have developed a technique to quantitatively and specifically measure $^{\bullet}OH$ in aqueous solutions such as in a surrogate for lung fluid. While prior studies have investigated $^{\bullet}OH$ formation by ambient PM containing transition metals, this study presents quantitative measurement of $^{\bullet}OH$ formation by soot (with added HOOH) in the absence of transition metals. In this paper we examine four main questions: (1) Is $^{\bullet}OH$ generated by soot particles in a surrogate lung fluid (SLF)? (2) How does $^{\bullet}OH$ generation depend on the

amounts of soot and HOOH present? (3) How does the reactivity of flame soot compare with that of ambient fine particles and of Degussa carbon black, a commonly used surrogate for atmospheric soot in health effect studies (Brown et al., 2000)? (4) How important are transition metals in the formation of $^{\bullet}$OH from soot and ambient PM2.5?

2. Materials and methods

2.1. Chemicals

Benzoic acid (99.5%, ACS reagent) and deferox-amine mesylate (DSF) (approx. 95%, TLC) were obtained from Sigma, and p-hydroxybenzoic acid was obtained from TCI America. All other chemicals were from Fisher (certified ACS or optima grade). Standard solutions of metals in 2% nitric acid for ICP-MS analysis were from SPEX. Purified water ("Milli-Q water") was obtained from a Milli-Q Plus system (Millipore; $\geqslant 18.2 \, M\Omega \, cm$).

2.2. Particle generation and collection

We generated soot particles with a co-flow, laminar, diffusion flame system. Ethylene was used as fuel at 0.493 slpm to generate soot aerosol at a sooting flame condition. Soot particles were cooled and diluted after emission by mixing with HEPA filtered, co-flowing air. The typical total sampling flow rate was 24 lpm for three simultaneously collected filters (pre-weighed Teflon membranes; $\phi 47 \, mm$, 200 nm pore size, Advantec MFS Inc.) held in aluminum filter holders ($\phi 47 \, mm$; Pall Co.) to prevent contamination of samples by transition metals such as iron. In addition, we replaced the original stainless steel support screen in each filter holder with an aluminum screen and used aluminum fittings and tubing. Each filter was weighed after collection using a weak ionization source (Static Master, NRD) to eliminate static charges from the filters in order to get more accurate sample weights. A test showed that the influence of this static charge was only important for samples with masses less than $\sim 2 \, mg$.

Particle size distributions were measured using the same sampling probe with a scanning mobility particle sizer (TSI Inc.). Size distributions were lognormal with a geometric mean diameter of 185 nm (GSD = 1.539).

Ambient PM2.5 samples were collected using IMPROVE Version II Particulate Air Pollution Samplers (URG) containing Teflo filters (25 mm, pore size 3 μm, Pall Co.). We collected duplicate samples using the same condition for the master and slave sampling modules. Twenty-four hours of sampling at a flow rate of 23 lpm yielded 0.10–0.45 mg of collected particles.

2.3. Surrogate lung fluid (SLF)

As a simple surrogate for lung fluid (Davies and Feddah, 2003; Moss, 1979) we used a buffered aqueous solution containing 114 mM NaCl, 31 mM NaHCO$_3$, 10 mM total phosphate (3.6 mM Na$_2$HPO$_4$ and 6.4 mM KH$_2$PO$_4$ to buffer the solution at pH 7.4), 10 mM of benzoate (BA) as an $^{\bullet}$OH scavenger and typically 1.0 mM of HOOH. Based on kinetic calculations, this amount of BA should scavenge >99% of the $^{\bullet}$OH formed in the regular SLF extractions and only slightly less (>95%) in the SLF extractions with added DSF. SLF solutions without HOOH were kept in a refrigerator between experiments and were used within 3 weeks. HOOH was added into the SLF immediately prior to particle extraction.

2.4. Particle extraction

We typically extracted samples within a day after collection, but we also found that storing the sampled filters in plastic containers for 6 days on a lab bench caused no significant change in $^{\bullet}$OH generation. Particle suspensions were prepared by putting either a whole, half, or quarter filter in a 125 ml HDPE (or 20 ml PP) bottle containing 10 ml (or 5 ml) of SLF and shaking them for 2 h on a shake table at room temperature. Suspensions were filtered using a syringe (3 ml Norm-Ject, Henke Sass Wolf Gmbh) with a 0.22 μm syringe filter (Millex$^{\circledR}$GP, Millipore). Each day we extracted one blank, unsampled filter using the same method to determine our background signal. In addition to shaking, we also examined sonication as a means to extract particles from filters, but found that this method generated $^{\bullet}$OH: 30 min of sonication of 5 ml of SLF solution without added particles produced 5.6 nmol of $^{\bullet}$OH if the sonication water bath was not temperature controlled (maximum of $\sim 50\,^{\circ}C$ during the extraction) and 0.29 nmol of $^{\bullet}$OH if the bath was kept at $\sim 0\,^{\circ}C$ with ice. Compared to the amounts of $^{\bullet}$OH generated by our samples (see Section 3), this $^{\bullet}$OH radical generation by sonication is significant and therefore we used only shaking for particle extraction.

We also extracted portions of sampled filters with 3% HNO_3 or SLF by shaking in HDPE bottles for 2 h, followed by syringe filtering, to obtain samples for trace metal analysis by ICP-MS. To each 4 ml extract we added 200 μl of 500 ppb yttrium solution as an internal standard. Extracts in SLF were diluted by a factor of 10 or 20 to reduce the amount of total dissolved salts/solids (TDS) from ~1% to the recommended maximum of 0.1% for our ICP-MS analysis. Extracts in 3% HNO_3 were used without further dilution. The average limit of detection (LOD) ± 1 standard deviation, determined as three times the value of the blank solutions (Milli-Q with 3% nitric acid), was 58 ± 47 nM for iron and 13 ± 12 nM for the other transition metals.

2.5. Measurement of $^{\bullet}OH$ formation using high-performance liquid chromatography (HPLC)

$^{\bullet}OH$ was quantitatively trapped and measured using a BA chemical probe technique modified somewhat from previous studies (Anastasio and McGregor, 2001; Zhou and Mopper, 1990). In this technique $^{\bullet}OH$ reacts quantitatively with BA to form p-hydroxybenzoate (p-HBA) that is quantified by HPLC:

$$BA + {}^{\bullet}OH \rightarrow p\text{-HBA} + \text{other products.} \quad (2)$$
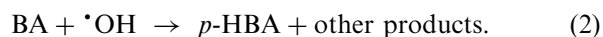
For our samples we typically acidified 2 ml of filtered extract (soon after filtration) to pH 2 (using 72 μl of 1 M H_2SO_4) in order to protonate p-HBA to its acid form, p-hydroxybenzoic acid, which is easier to determine on the HPLC. The acidified extract was then shaken and immediately injected into the HPLC for measurement of p-HBA. We took care to avoid exposure of the extract to metals as much as practical: an all-plastic syringe was used for filtering, a Teflon syringe needle was used to draw extracts into an all-glass syringe, and then the Teflon needle was replaced with a blunt, stainless steel HPLC needle only immediately prior to injection on the HPLC.

The HPLC used in this study consisted of a Shimadzu LC10-AT pump, a Keystone Scientific C-18 Beta Basic reverse-phase column (250×3 mm, 5 μm bead) with attached guard column, and a Shimadzu SPD-10AV UV/Visible detector ($\lambda = 256$ nm). The eluent was 30% CH_3CN/70% H_2O adjusted to pH 2 with $HClO_4$ at a flow rate of 0.60 ml min^{-1}. p-HBA was determined based on calibration standards made in SLF and run during

the day of the experiment, approximately 1 h after preparation and addition of HOOH.

We determined concentrations of p-HBA formed in a given sample by subtracting the blank signal from the sample signal:

$$[p\text{-HBA}] = [p\text{-HBA}]_{\text{sample}} - [p\text{-HBA}]_{\text{blank}}. \quad (3)$$

The blank concentration was measured using a blank filter that was treated exactly like a sample (extraction, filtration, and acidification) on the same day of the experiment. Concentrations of $^{\bullet}OH$ were then calculated using

$$[{}^{\bullet}OH] = [p\text{-HBA}]/Y_{p\text{-HBA}}, \quad (4)$$

where $Y_{p\text{-HBA}}$ is the yield of p-HBA from the reaction of $^{\bullet}OH$ with BA in SLF (0.215 ± 0.018, $n = 2$). This value of $Y_{p\text{-HBA}}$ in SLF was determined in the same manner described previously (Anastasio and McGregor, 2001) and is very similar to the value (0.17 ± 0.0017) determined in Milli-Q water in this past study. Concentrations of $^{\bullet}OH$ were converted to an absolute amount of $^{\bullet}OH$ formed per mass of PM sample using

$${}^{\bullet}OH \text{ (nmol mg}^{-1}) = [{}^{\bullet}OH \text{ (μM)}] \times \text{SLF extract}$$
$$\text{volume (l)} \times 1000/\text{sample mass (mg).} \quad (5)$$

3. Results

3.1. $^{\bullet}OH$ formation as a function of soot particle mass

As illustrated in Fig. 1, $^{\bullet}OH$ was formed from all of our soot samples, even filters containing as little as 1 mg of soot. The amount of $^{\bullet}OH$ formed in the extraction solution was linearly dependent on soot mass up to the maximum amount tested (30 mg).
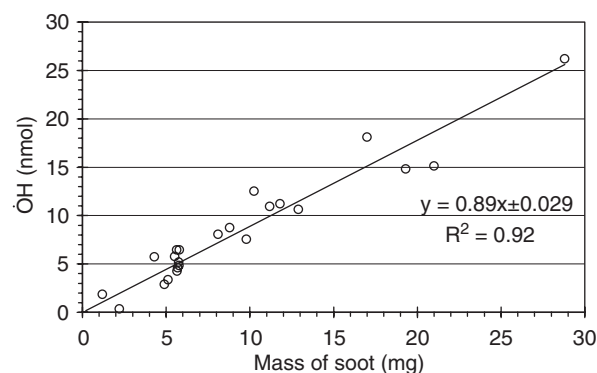

$$y = 0.89x \pm 0.029$$
$$R^2 = 0.92$$

Fig. 1. Formation of hydroxyl radical from different masses of flame soot particles extracted into a surrogate lung fluid.

The average (± 1 SE) response from these samples is 0.89 nmol (± 0.029) $^{\bullet}$OH produced per mg of soot, as determined from a linear regression slope (with a fixed intercept of zero) in Fig. 1. This linearity suggests a stoichiometric reaction between HOOH and soot and indicates that the amount of soot is limiting the reaction under these conditions (i.e., with 1.0 mM HOOH). Note that there is no threshold for $^{\bullet}$OH formation at low soot concentrations in Fig. 1: the y-intercept (± 1 SE) from the linear regression of the data is 0.37 (± 0.56) which is insignificantly different from zero (p-value $= 0.255$). Although we find a linear relationship between $^{\bullet}$OH generation and soot mass this does not necessarily mean that $^{\bullet}$OH is derived from the particle volume (e.g., rather than from the surface). Since our samples had a fixed particle size distribution the particle surface area is approximately directly proportional to soot mass.

3.2. $^{\bullet}$OH formation as a function of hydrogen peroxide concentration

We have also characterized how the amount of $^{\bullet}$OH formed depends on the concentration of HOOH (0–1 mM) in the SLF. Previous studies have employed a wide range of HOOH concentrations, ranging from 1.5×10^{-4} to 1 mol HOOH per gram of sample (Dellinger et al., 2001; Shi et al., 2003; Valavanidis et al., 2000; van Maanen et al., 1999). The lower end of this range is similar to the mass-normalized amounts of HOOH produced by human neutrophils exposed to PM, where 50 or 100 μg ml^{-1} of ambient PM produced $\sim$5–6 μM of HOOH, i.e., a production of $(0.5–1.2) \times 10^{-4}$ mol HOOH per gram of particles (Kinnula et al., 1991; Knaapen et al., 2002). Our concentration of 1.0 mM of HOOH for 1–30 mg of soot is equivalent to 3.3×10^{-4} to 10^{-2} mol HOOH per gram of sample.

We used quarter filters containing 5 mg of flame soot for these experiments. As shown in Fig. 2, there was no detectable $^{\bullet}$OH formation in the absence of HOOH, indicating that it is the interaction of soot with HOOH that forms $^{\bullet}$OH. $^{\bullet}$OH formation increased steadily up to approximately 0.2 mM of added HOOH and reached a plateau at $\sim$0.5 mM HOOH. To insure that $^{\bullet}$OH generation in our other experiments was not limited by HOOH we used 1.0 mM HOOH in the SLF.

At low concentrations of HOOH it appears that the formation of $^{\bullet}$OH is limited by the availability of HOOH, while at the plateau the reaction is
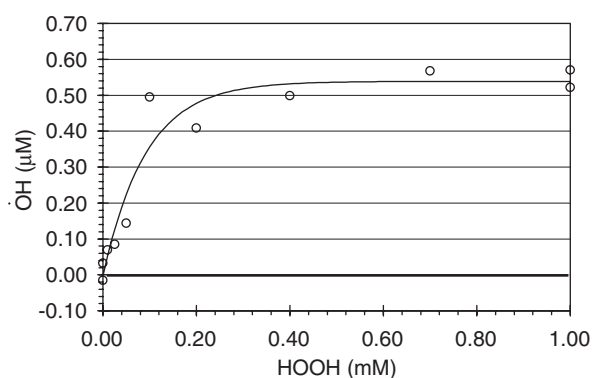

Fig. 2. Effect of HOOH concentration on the amount of hydroxyl radical formed from 5 mg of flame soot particles extracted into the aqueous extract solution containing 10 mM BA and variable concentrations of hydrogen peroxide. The solid line represents a regression fit to the data: $[^{\bullet}OH] = -3.7 \times 10^{-3}$ (± 0.040) $+ 0.54$ (± 0.050) $\times (1 - \exp(-11$ (± 3.1) $\times [HOOH]))$ where uncertainties are ± 1 SE and $R^2 = 0.94$.

limited by the amount of soot. However, we cannot rule out that the smaller $^{\bullet}$OH responses at low concentrations of HOOH are due to slower reaction rates since we extracted all samples for 2 h. The initial slope (± 1 SE) of the regression line to the experimental data (i.e., d[OH]/d[HOOH] at [HOOH]$\rightarrow 0$) is $(5.9 \pm 2.2) \times 10^{-3}$. This indicates that 0.59% of the HOOH molecules are converted to $^{\bullet}$OH at low concentrations of HOOH. This low apparent yield suggests that most of the reactions between reactive soot moieties and HOOH result in products other than $^{\bullet}$OH.

3.3. Extraction time course experiment

$^{\bullet}$OH in our experiments is formed by a reaction between soot and HOOH in the SLF. This reaction likely depends upon both a physical extraction process (e.g., the mobilization of reactive soot "sites" to the surface of the soot or into the solution) as well as the kinetics of the chemical reaction between the reactive "sites" and HOOH. It is possible that either of these processes could control the amount of $^{\bullet}$OH formed in a given time. To examine the rates of this coupled extraction/reaction system in our experiments and to determine the appropriate extraction time for our experiments we conducted a series of time course experiments. To do this we prepared triplicate samples each containing 20 (± 1) mg of soot from the same flame condition then cut each filter into quarters. SLF was added to each quarter filter and the mixture was

extracted for known times and then analyzed for *p*-HBA.

Fig. 3 shows the resulting •OH concentrations (normalized by sample mass) as a function of extraction time. The time constant (for 63% rise) was 17 min for this fit, while extraction and/or reaction were complete in about 90 min as shown in Fig. 3. For the rest of our experiments particles were extracted for 2 h to assure complete extraction/reaction.

3.4. Role of Fe and other transition metals: Part I (metal concentrations measurements)

Past studies of •OH generation by particles (either in ambient air or emitted from specific sources) have focused on the role of transition metals, especially iron. However, because we produce our particles using an ethylene flame we expect that there will be only trace levels of iron and other transition metals in the resulting particles. To examine this, we have measured the concentrations of several transition metals (Fe, Cu, V, Cr, Mn, and Ni) in nitric acid extracts of a subset ($n = 4$) of our particle samples using ICP-MS.

While Fe in our nitric acid extracts was present at levels above the LOD (58 ± 47 nM), concentrations of the other metals were below their LODs (13 ± 12 nM). We expect that the concentrations of these species in the corresponding SLF extracts (at pH 7.4) would be even lower since nitric acid is better at dissolving metals. We measured transition metals in the SLF extracts, but these samples were not useful since they needed to be diluted by factors
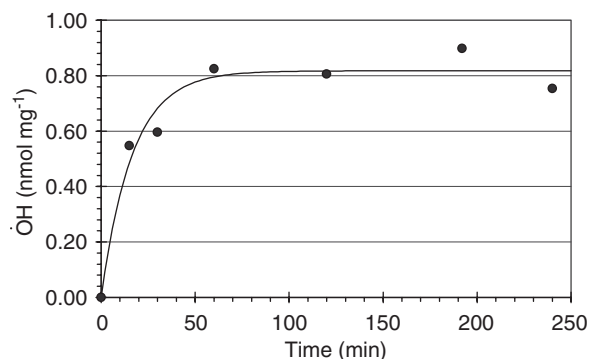
of 10 or 20 (in order to reduce the level of TDS for ICP-MS), raising detection limits by the same factors.

The average ($\pm 1\,\sigma$) iron concentration in the four samples in which we measured transition metals was 305 ± 172 nM. However, there was a negative correlation between the amount of •OH generated by a sample in SLF and the amount of Fe measured in the corresponding nitric acid extracts (slope $\pm$ SE $= -0.52 \pm 0.0069$; $n = 4$), suggesting that the very low amounts of Fe did not participate in •OH generation. Based on the addition of Fe(II) in SLF, where 20 µM of $FeSO_4$ generated 5.6 nmol •OH (see below), we calculate that the measured amounts of iron in the soot samples would have produced $\leqslant 0.085$ nmol of •OH, much less than the amounts of measured •OH (Fig. 1).

3.5. Role of Fe and other transition metals: Part II (transition metal chelation)

To further investigate the possible role of iron and other transition metals in •OH generation from our soot samples we performed a number of experiments using desferrioxamine mesylate (DSF), a well-known transition metal chelator (Shi et al., 2003). We used four different experimental conditions for a given set of soot samples: (1) soot only (as described previously), (2) soot treated with DSF prior to SLF extraction, (3) soot with added Fe(II) (as $FeSO_4$), and (4) soot with added Fe(II) and DSF prior to extraction. For each condition we used a quarter of a filter that (whole) contained a total of 20 (± 1) mg of soot. For condition (1) we used the same procedure as described previously. For the other conditions (2)–(4), 1 ml of a 20 µM Fe(II) and/or 1 ml of a 3.2 mM DSF solution was added to the soot filter in a 20 ml (Nalgene, PP) bottle and the sample was shaken for 30 min on a shake table. Next, 5 ml of SLF was added, the sample was extracted for 2 h on a shake table, and then the extract was treated as described previously. A blank experiment where 1 ml Milli-Q was added to a sample prior to SLF extraction confirmed that the increase of volume by 1 ml does not affect the •OH results except for the minor amount of dilution, which is taken into account in our calculations.

Fig. 4 shows the results from the above experiments. The •OH response from the plain soot, 0.42 (± 0.078) nmol mg^{-1}, is smaller than that from Fig. 1 (0.89 ± 0.029), perhaps because the smaller

Fig. 3. Formation of hydroxyl radical from 5 mg of flame soot particles extracted into a surrogate lung fluid as a function of extraction time (*t*). The solid line represents a regression fit to the data: •OH $= 0.82$ (± 0.036) $\times (1 - \exp(-0.060$ ($\pm 0.012) \times t))$ where uncertainties are ± 1 SE and $R^2 = 0.96$.
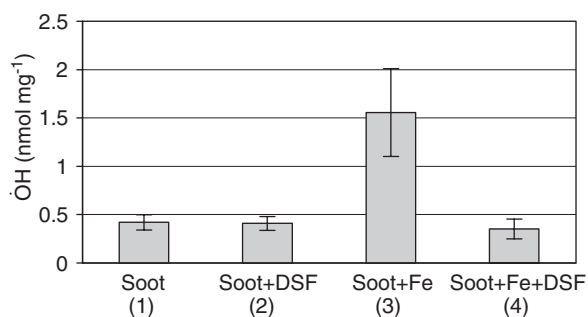
Fig. 4. Effect of an iron chelator (DSF) on the generation of
$^{\bullet}$OH from flame soot particles.

bottle resulted in less efficient extraction/reaction of
the soot. In any case, the $^{\bullet}$OH response for this
untreated soot was the same (within experimental
uncertainties) for the soot that had been pretreated
with DSF (experiment (2)). This indicates that iron
and other transition metals (which will be chelated
by DSF) are insignificant sources of $^{\bullet}$OH in our
soot experiments, suggesting that carbonaceous
soot components are responsible for $^{\bullet}$OH genera-
tion in the presence of HOOH. To confirm that Fe
produces a response in our experiments we per-
formed experiment (3) as a positive control, by
adding 20 μM of Fe(II) to the soot before extracting
with SLF. As shown in Fig. 4, this amount of Fe
produced a large increase in $^{\bullet}$OH, equivalent to
0.95 μM $^{\bullet}$OH in the 6 ml of solution, which
indicates that the efficiency of $^{\bullet}$OH production
from the Fenton reaction under these conditions is
4.8%. Finally, experiment (4) with soot, Fe(II), and
DSF shows that the additional $^{\bullet}$OH formed from
the Fe(II) is suppressed (as we expect from DSF)
but that the $^{\bullet}$OH amount formed by the soot
remains unchanged. These results, especially in
conjunction with the ICP-MS results, indicate that
$^{\bullet}$OH generated from our soot samples are from the
carbonaceous soot and not by trace amounts of Fe
or other transition metals.

3.6. Carbon black vs. flame soot

Carbon black is a widely used surrogate for flame
soot in health studies. While carbon black is a
convenient, readily purchased chemical with a well
defined, standard method for production for each
specific product (e.g., Printex-U from Degussa), a
potential problem with using carbon black is that its
reactivity and surface properties are likely to be
different from those of flame soot, which better

simulates ambient carbon particles from various
combustion sources for health studies. To examine
this issue for ROS generation we compare the
reactivity of soot particles with those of carbon
black in terms of $^{\bullet}$OH generation in SLF. In our
experiments we extracted 5–10 mg of carbon black
in SLF using the procedure described in Section 2.4.
Note that carbon black and flame soot have
different physical and chemical properties. For
example, the BET surface area and mean primary
particle size are 300 $m^2 g^{-1}$ and 14 nm, respectively,
for carbon black (data from Degussa) while values
are 120 $m^2 g^{-1}$ and 25 nm, respectively, for flame
soot (Stanmore et al., 2001). Based on our TEM
image of the flame soot (data not shown) and the
image of Degussa Printex-U carbon black from
Stone et al. (1998), the morphologies of these
particle types are similar except for the difference
in primary particle size. Furthermore, the amounts
of nitric-acid extractable Fe are 3.8 nmol mg^{-1} for
carbon black and <0.05 nmol mg^{-1} for flame soot
based on our ICP-MS measurements. Finally, based
on data from the manufacturer, the ash content of
the carbon black is 0.4% and the amount of volatile
matter at 950 °C is 1%.

As with flame soot, we find that $^{\bullet}$OH generation
by carbon black is also linearly proportional to PM
mass, but carbon black is much less efficient at
generating $^{\bullet}$OH. Fig. 5 shows that, on a mass basis,
carbon black generates approximately one-tenth as
much $^{\bullet}$OH compared to flame soot. Possible
reasons for this difference in reactivity could be
differences in the physical and chemical properties
of the two types of particles. However, as described
above, carbon black has both a larger BET surface
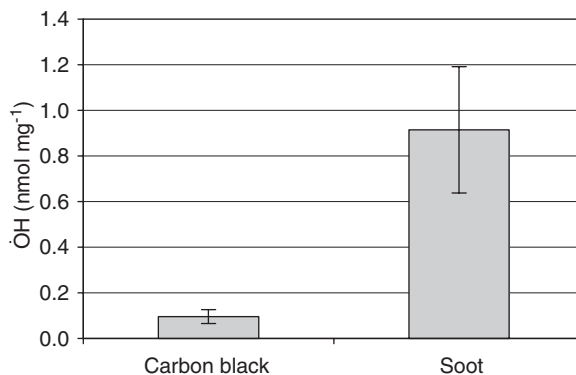area than flame soot as well as over 70 times more

Fig. 5. Comparison of the average ($\pm 1~\sigma$), mass-normalized
$^{\bullet}$OH generation (from flame soot (0.91$\pm$0.28 nmol mg^{-1}) and
Degussa carbon black (0.096$\pm$0.030 nmol mg^{-1})).

nitric acid-extractable Fe than flame soot. Both of these factors suggest that carbon black should be more reactive, in contrast to the experimental results. This indicates that other factors (e.g., soot structure and different concentrations or speciation of organic carbon components) are controlling the $^\bullet$OH reactivity.

3.7. $^\bullet$OH formation by ambient PM2.5

Our final goals are to quantify the amounts of $^\bullet$OH produced from ambient fine particles (PM2.5) and determine whether a portion of this ROS generation is via mechanisms that do not involve transition metals. Fig. 6 shows the $^\bullet$OH response from ambient PM2.5 collected in Davis, California, with and without pretreatment with the transition metal chelator DSF. PM2.5 samples without DSF pretreatment (samples A–D) show that there is significant variability (by a factor of $\sim$6) in the mass-normalized production of $^\bullet$OH on different sampling days, indicating that there is a wide range of particle compositions and reactivities even on just these few days. The ambient samples also have much greater (by factors of 6–36) mass-normalized $^\bullet$OH generation compared to flame soot. In the two samples where replicate filters were pretreated with the iron chelator (C+DSF and D+DSF) much of the $^\bullet$OH responses were suppressed, but a significant fraction of $^\bullet$OH generation remained (43% and 12% for samples C and D, respectively). This
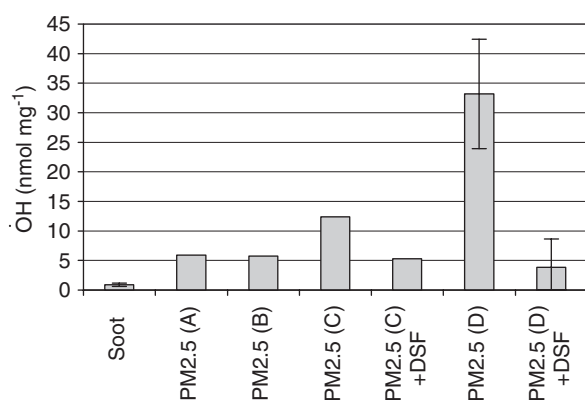
fraction of $^\bullet$OH generation by ambient PM is not from transition metals but could be from carbonaceous soot. Mass-normalized concentrations (nmol mg^{-1}) of transition metals in 3% nitric acid extracts of samples B and D are, respectively, 103 and 80 for Fe, 1.5 and 18 for Cu, 6 and 1 for Mn, <0.042 and 1.3 for Ni, <0.19 and <0.7 for Cr, and <0.17 and <0.05 for V. While these data are limited because we do not know the oxidation states of the metals, they suggest that Fe and Cu, the most abundant metals, are most important for $^\bullet$OH generation in these PM2.5 samples. Based on the 4.8% efficiency for $^\bullet$OH formation from Fe(II) that we determined from the data in Fig. 4, we expect that the Fe in sample D would produce $\sim$4 nmol mg^{-1} of $^\bullet$OH (assuming it is all Fe(II)). The fact that this sample has a DSF-inhibitable $^\bullet$OH signal of $\sim$30 nmol mg^{-1} suggests either that the Fe is recycled by reductants back to reactive Fe(II) after it participates in the Fenton reaction (Ball et al., 2000; Dellinger et al., 2000, 2001) or that Cu plays a large role in $^\bullet$OH generation in this sample.

These preliminary results suggest that Fe, Cu, or other transition metals are a major cause of $^\bullet$OH generation by ambient PM, which is consistent with previous studies (Donaldson et al., 1997; Shi et al., 2003; van Maanen et al., 1999). However, these results also reveal that ambient particles generate significant amounts of $^\bullet$OH by pathways that do not involve transition metals, possibly by carbonaceous soot such as we have seen in our laboratory-generated samples.

4. Discussion

Here we assess the flux and potential significance of particle-generated $^\bullet$OH in lungs based on our results. Assuming 30 µg m^{-3} as a typical mass concentration of fine particles (Gray et al., 1986), a daily volume of $\sim$20 m^3 of inhaled air, and that $\sim$15% of these particles deposit to the lung (Friedlander and Yeh, 1998), we calculate a daily lung deposition of $\sim$90 µg of PM2.5 per person. This will generate $\sim$2 nmol $^\bullet$OH daily per person based on a response of 20 nmol $^\bullet$OH per mg of PM2.5 (Fig. 6).

This generation of $^\bullet$OH will be damped by antioxidants such as ascorbate, urate, and reduced glutathione, all of which are present in the lung lining fluid at concentrations of $\sim$200 µM (Greenwell et al., 2003). Based on an estimated

Fig. 6. Comparison of $^\bullet$OH generation from flame soot (from Fig. 1) and ambient fine particles (PM2.5) in the aqueous extract solution with 1.0 mM of HOOH. Samples were collected for $\sim$24 h on the following dates: (dd:mm:yy), A (27-9-04), B (29-9-04), C (9-2-05), D (17-2-05). The error bars on samples D and "D+DSF" represents $\pm$1 σ from triplicate samples collected at the same time in parallel collectors. The average generation of $^\bullet$OH from these PM2.5 samples is 21 ± 15 nmol mg^{-1}.

adult lung lining fluid volume of 25 ml (Walters, 2002), this corresponds to ~15 µmol of total antioxidant, which is much greater than the ~2 nmol of $^{\bullet}$OH estimated to be generated from PM2.5 deposition in the lungs. Despite this disparity the particle-mediated formation of $^{\bullet}$OH could still be biologically significant because of factors such as: (1) The presence of reductants in lung lining fluid, including ascorbate, will lead to additional $^{\bullet}$OH via the recycling of particle-derived precursors such as Fe(II) from Fe(III) (e.g., Ball et al., 2000). (2) While the antioxidant pool will lower the overall $^{\bullet}$OH pseudo-steady-state concentration, it will not intercept every $^{\bullet}$OH generated by PM (or other mechanisms). Thus some fraction of the $^{\bullet}$OH formed could still react with important biological molecules including DNA and cell membranes (Imlay et al., 1988; Imlay and Linn, 1988). (3) A portion of this $^{\bullet}$OH will react with lipids to cause peroxidation, which can lead to a self-propagating chain reaction where one $^{\bullet}$OH leads to the oxidation of many lipid molecules (e.g., Mylonas and Kouretas, 1999). (4) In addition, if the particles produce an immune response (e.g., from phagocytes) this can lead to additional reactive oxidants that are not generated in our cell-free SLF assay.

5. Conclusions

The formation of ROS in lungs is a plausible mechanism by which particles elicit toxic effects. Understanding how factors such as particle composition and surface area are related to the oxidation potential of PM requires that we can measure ROS quantitatively. To help address this need, we have developed a technique that can quantitatively measure the amount of $^{\bullet}$OH radical (the strongest biological oxidant) formed from particles in an aqueous extract solution as a simple surrogate for lung fluid. With this method we find that laboratory-generated soot from an ethylene flame (as a surrogate for combustion soot in the atmosphere) generates $^{\bullet}$OH radical in the absence of transition metals. This $^{\bullet}$OH formation exhibits a dose-dependent linear response with soot mass, which suggests that the reaction is stoichiometric and that the amount of soot limits the reaction under our conditions. We also found that carbon black, which is often used as a surrogate of soot in health effect studies, has a much lower reactivity than our flame soot in terms of $^{\bullet}$OH generation. Using the $^{\bullet}$OH technique on a few ambient PM2.5 samples reveals

that while transition-metal-dependent pathways for $^{\bullet}$OH are dominant, a significant fraction of the $^{\bullet}$OH generation is not caused by transition metals and could be due to carbonaceous components. From our PM2.5 results we estimate a particle-produced burden of pulmonary $^{\bullet}$OH of ~2 nmol $^{\bullet}$OH per person per day. Even though this is much smaller than the total antioxidant level in the lung lining fluid, the particle-mediated production of $^{\bullet}$OH could still be biologically significant, although more work is needed to evaluate this possibility.

References

Anastasio, C., McGregor, K.G., 2001. Chemistry of fog waters in California's central valley: 1. In situ photoformation of hydroxyl radical and singlet molecular oxygen. Atmospheric Environment 35, 1079–1089.

Ball, B.R., Smith, K.R., Veranth, J.M., Aust, A.E., 2000. Bioavailability of iron from coal fly ash: mechanisms of mobilization and of biological effects. Inhalation Toxicology 12 (Suppl. 4), 209–225.

Brown, D.M., Stone, V., Findlay, P., MacNee, W., Donaldson, K., 2000. Increased inflammation and intracellular calcium caused by ultrafine carbon black is independent of transition metals or other soluble components. Occupational and Environmental Medicine 57, 685–691.

Cohen, A.J., Higgins, M.W.P., 1995. Diesel exhaust: A critical analysis of emissions, exposure, and health effects. Health Effects Institute, 251–292.

Davies, N.M., Feddah, M.R., 2003. A novel method for assessing dissolution of aerosol inhaler products. International Journal of Pharmaceutics 225, 175–187.

Dellinger, B., Pryor, W.A., Cueto, R., Squadrito, G., Deutsch, W.A., 2000. The role of combustion-generated radicals in the toxicity of PM2.5. Proceedings of the Combustion Institute 28, 2675–2681.

Dellinger, B., Pryor, W.A., Cueto, R., Squadrito, G.L., Hegde, V., Deutsch, W.A., 2001. Role of free radicals in the toxicity of airborne fine particulate matter. Chemical Research in Toxicology 14, 1371–1377.

Dockery, D.W., Pope III, C.A., Xu, X., Spengler, J.D., Ware, J.H., Fay, M.E., Ferris, B.G., Speizer, F.E., 1993. An association between air pollution and mortality in six U.S. cities. New England Journal of Medicine 329, 1753–1759.

Donaldson, K., Brown, D.M., Mitchell, C., Dineva, M., Beswick, P.H., Gilmour, P., MacNee, W., 1997. Free radical activity of PM10: iron-mediated generation of hydroxyl radicals. Environmental Health Perspectives 105, 1285–1289.

Friedlander, S.K., Yeh, E.K., 1998. The submicron atmospheric aerosol as a carrier of reactive chemical species: case of peroxide. Applied and Occupational Environmental Hygiene 13, 416–420.

Gray, H.A., Cass, G.R., 1998. Source contributions to atmospheric fine carbon particle concentrations. Atmospheric Environment 32, 3805–3825.

Gray, H.A., Cass, G.R., Huntzicker, J.J., Heyerdahl, E.K., Rau, J.A., 1986. Characteristics of atmospheric organic and elemental carbon particle concentrations in Los-Angeles. Environmental Science and Technology 20, 580–589.

Greenwell, L.L., Moreno, T., Richards, R.J., 2003. Pulmonary antioxidants exert differential protective effects against urban and industrial particulate matter. Journal of Biosciences 28, 101–107.

Han, J.Y., Takeshita, K., Utsumi, H., 2001. Noninvasive detection of hydroxyl radical generation in lung by diesel exhaust particles. Free Radical Biology and Medicine 30, 516–525.

Imlay, J.A., Linn, S., 1988. DNA damage and oxygen radical toxicity. Science 240, 1302–1309.

Imlay, J.A., Chin, S.M., Linn, S., 1988. Toxic DNA damage by hydrogen peroxide through the Fenton reaction in vivo and vitro. Science 240, 640–642.

Kinnula, V.L., Everitt, J.I., Whorton, A.R., Crapo, J.D., 1991. Hydrogen peroxide production by alveolar type II cells, alveolar macrophages and endothelial cells. American Journal of Physiology 261, L84–L91.

Knaapen, A.M., Shi, T.M., Borm, P.J.A., Schins, R.P.F., 2002. Soluble metals as well as the insoluble particle fraction are involved in cellular DNA damage induced by particulate matter. Molecular and Cellular Biochemistry 234, 317–326.

Li, N., Sioutas, C., Cho, A., Schmitz, D., Misra, C., Sempf, J., Wang, M., Oberley, T., Froines, J., Nel, A., 2003. Ultrafine particulate pollutants induce oxidative stress and mitochondrial damage. Environmental Health Perspectives 111, 455–460.

McClellan, R.O., 1987. Health-effects of exposure to diesel exhaust particles. Annual Review of Pharmacology and Toxicology 27, 279–300.

Moss, O.R., 1979. Simulants of lung interstitial fluid. Health Physics 36, 447–448.

Mylonas, C., Kouretas, D., 1999. Lipid peroxidation and tissue damage. In Vivo 13, 295–309.

Puxbaum, H., Wopenka, B., 1984. Chemical-composition of nucleation and accumulation mode particles collected in Vienna, Austria. Atmospheric Environment 18, 573–580.

Sagai, M., Lim, H.B., Ichinose, T., 2000. Lung carcinogenesis by diesel exhaust particles and the carcinogenic mechanism via active oxygens. Inhalation Toxicology 12, 215–223.

Samet, J.M., Dominici, F., Curriero, F.C., Coursac, I., Zeger, S.L., 2000. Fine particulate air pollution and mortality in 20 U.S. cities, 1987–1994. New England Journal of Medicine 343, 1742–1749.

Shi, T., Schins, R.P.F., Knaapen, A.M., Kuhlbusch, T., Pitz, M., Heinrich, J., Borm, P.J.A., 2003. Hydroxyl radical generation by electron paramagnetic resonance as a new method to monitor ambient particulate matter composition. Journal of Environmental Monitoring 5, 550–556.

Stanmore, B.R., Brilhac, J.F., Gilot, P., 2001. The oxidation of soot: a review of experiments, mechanisms and models. Carbon 39, 2247–2268.

Stone, V., Shaw, J., Brown, D.M., MacNee, W., Faux, S.P., Donaldson, K., 1998. The role of oxidative stress in the prolonged inhibitory effect of ultrafine carbon black on epithelial cell function. Toxicology in Vitro 12, 649–659.

Valavanidis, A., Salika, A., Theodoropoulou, A., 2000. Generation of hydroxyl radicals by urban suspended particulate air matter. The role of iron ions. Atmospheric Environment 34, 2379–2386.

van Maanen, J.M.S., Borm, P.J.A., Knaapen, A., van Herwijnen, M., Schilderman, P., Smith, K.R., Aust, A.E., Tomatis, M., Fubini, B., 1999. In vitro effects of coal fly ashes: hydroxyl radical generation, iron release, and DNA damage and toxicity in rat lung epithelial cells. Inhalation Toxicology 11, 1123–1141.

Walters, D.V., 2002. Lung lining liquid—the hidden depths. The fifth Nils W Svenningsen Memorial Lecture. Biology of the Neonate 81, 2–5.

Winterbourn, C.C., 1995. Toxicity of iron and hydrogen peroxide: the Fenton reaction. Toxicology Letters 82/83, 969–974.

Zhou, X., Mopper, K., 1990. Determination of photochemically produced hydroxyl radical in seawater and freshwater. Marine Chemistry 30, 71–88.